Biowire: a platform for maturation of human pluripotent stem cell–derived cardiomyocytes

Sara S Nunes[1,2], Jason W Miklas[1,13], Jie Liu[3,13], Roozbeh Aschar-Sobbi[3], Yun Xiao[1], Boyang Zhang[1], Jiahua Jiang[4], Stéphane Massé[5], Mark Gagliardi[6], Anne Hsieh[1], Nimalan Thavandiran[1], Michael A Laflamme[7], Kumaraswamy Nanthakumar[5], Gil J Gross[4,8–10], Peter H Backx[3,10,11], Gordon Keller[6] & Milica Radisic[1,10,12]

Directed differentiation protocols enable derivation of cardiomyocytes from human pluripotent stem cells (hPSCs) and permit engineering of human myocardium *in vitro*. However, hPSC-derived cardiomyocytes are reflective of very early human development, limiting their utility in the generation of *in vitro* models of mature myocardium. Here we describe a platform that combines three-dimensional cell cultivation with electrical stimulation to mature hPSC-derived cardiac tissues. We used quantitative structural, molecular and electrophysiological analyses to explain the responses of immature human myocardium to electrical stimulation and pacing. We demonstrated that the engineered platform allows for the generation of three-dimensional, aligned cardiac tissues (biowires) with frequent striations. Biowires submitted to electrical stimulation had markedly increased myofibril ultrastructural organization, elevated conduction velocity and improved both electrophysiological and Ca^{2+} handling properties compared to nonstimulated controls. These changes were in agreement with cardiomyocyte maturation and were dependent on the stimulation rate.

As adult human cardiomyocytes are essentially postmitotic, the ability to differentiate cardiomyocytes from human embryonic stem cells (hESCs) and human induced pluripotent stem cells (hiPSCs)[1–4] represents an exceptional opportunity to create *in vitro* models of healthy and diseased human cardiac tissues that can also be patient-specific[5] and useful in screening new therapeutic agents for efficacy. However, differentiated cells exhibit a low degree of maturation[6] and are appreciably different from adult cardiomyocytes.

hESC-derived cardiomyocytes exhibit immature sarcomere structure characterized by the absence of H zones, I bands and M lines (day 40 embryoid bodies[7]), high proliferation rates (~17% proliferating cells for day 37 embryoid bodies[8] (EBd37) and ~10% for day 21–35 embryoid bodies[7]), immature action potentials[9] and Ca^{2+} handling properties[9–13] with contraction shown to be, in many cases, dependent on trans-sarcolemmal Ca^{2+} influx and not on sarcoplasmic reticulum Ca^{2+} release[10]. hESC-based engineered cardiac tissues also exhibit characteristics of immature cells, including immature sarcomere structure[14], high proliferation rates (15–45% proliferating cells in ref. 14 and 10–30% proliferating cells in ref. 15) and expression of the fetal gene program[16–18]. This is an important caveat when using these cells as models of adult human tissue[6].

During embryonic development, cardiac cells are exposed to environmental cues such as extracellular matrix, soluble factors, mechanical signals and electrical fields that may determine the emergence of spatial patterns and aid in tissue morphogenesis[19,20]. Exogenously applied electrical stimulation has also been shown to influence cell behavior[21–23].

We created a platform that combines architectural and electrical cues to generate a microenvironment conducive to maturation of three-dimensional (3D) hESC-derived and hiPSC-derived cardiac tissues, termed 'biowires'. We seeded cells in collagen gel around a template suture in a microfabricated well and subjected them to electrical field stimulation with a progressive increase in frequency. Consistent with maturation, stimulated biowires exhibited cardiomyocytes with a remarkable degree of ultrastructural organization, improved conduction velocity and enhanced Ca^{2+} handling and electrophysiological properties.

RESULTS

Engineering of human cardiac biowires

We generated 3D, self-assembled cardiac biowires by seeding cardiomyocytes, derived from hPSCs using a directed differentiation protocol in embryoid bodies[2], and supporting cells

[1]Institute of Biomaterials and Biomedical Engineering, University of Toronto, Toronto, Ontario, Canada. [2]Toronto General Research Institute, University Health Network, Toronto, Ontario, Canada. [3]Department of Physiology and Medicine, University of Toronto, Toronto, Ontario, Canada. [4]Cardiology Division, Hospital for Sick Children, Toronto, Ontario, Canada. [5]The Toby Hull Cardiac Fibrillation Management Laboratory, Toronto General Hospital, Toronto, Ontario, Canada. [6]McEwen Centre for Regenerative Medicine, University Health Network, Toronto, Ontario, Canada. [7]Department of Pathology, University of Washington, Seattle, Washington, USA. [8]Physiology and Experimental Medicine Program, Hospital for Sick Children Research Institute, Toronto, Ontario, Canada. [9]Department of Pediatrics, University of Toronto, Toronto, Ontario, Canada. [10]The Heart and Stroke/Richard Lewar Centre of Excellence, Toronto, Ontario, Canada. [11]Division of Cardiology, University Health Network, Toronto, Ontario, Canada. [12]Department of Chemical Engineering and Applied Chemistry, University of Toronto, Toronto, Ontario, Canada. [13]These authors contributed equally to this work. Correspondence should be addressed to M.R. (m.radisic@utoronto.ca).

RECEIVED 6 FEBRUARY; ACCEPTED 17 MAY; PUBLISHED ONLINE 23 JUNE 2013; DOI:10.1038/NMETH.2524

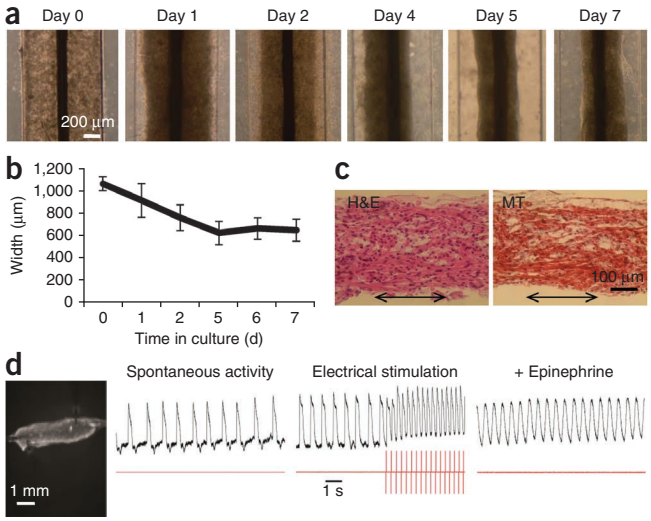

Figure 1 | Generation of human cardiac biowires. (**a**) Brightfield images of Hes2 hESC-derived cardiomyocytes on indicated days of preculture in biowire template. (**b**) Quantification of gel compaction on the indicated days of culture (average ± s.d., $n = 3$ (day 0), $n = 4$ (days 1–7)). (**c**) Hematoxylin and eosin (H&E) and Masson's trichrome (MT) staining of biowire sections (double-headed arrows represent suture axis). (**d**) Representative picture (left) of a biowire being imaged with potentiometric fluorophore (DI-4-ANEPPS), which shows spontaneous electrical activity, with impulse propagation recording (left trace recording), response to electrical stimulation (middle trace recording, stimulation frequency is depicted in red trace below) and increase in frequency of spontaneous response under pharmacological stimulation (epinephrine, right trace recording).

(fibroblasts, endothelial cells and smooth muscle cells) into a template poly(dimethylsiloxane) (PDMS) channel, around a sterile surgical suture in type I collagen gels (**Fig. 1** and **Supplementary Fig. 1a**). The biowire suture remained anchored to the device platform during matrix remodeling. Seeded cells remodeled and contracted the collagen gel matrix during the first week after seeding (**Fig. 1a** and **Supplementary Fig. 1a**) with ~40% gel compaction (**Fig. 1b**; final width, ~600 μm). This allowed us to remove the biowire from the PDMS template (**Supplementary Figs. 1** and **2**).

Histological analysis revealed cell alignment along the axis of the suture (**Fig. 1c** and **Supplementary Fig. 2b**). Biowires beat synchronously and spontaneously between 2 d and 3 d after seeding and kept beating after gel compaction, demonstrating that the setup enabled electromechanical cell coupling (**Supplementary Video 1**). Biowires could be electrically paced and responded to physiological agonists such as epinephrine (β-adrenergic stimulation) by increasing frequency of spontaneous beating (**Fig. 1d**).

After preculture for 1 week, we either submitted the biowires to electrical field stimulation or cultured them without stimulation (nonstimulated controls) for 7 d. To assess whether effects were dependent on stimulation rate, we used two different protocols: (i) low-frequency ramp-up regimen, where stimulation started at 1 Hz, increased to 3 Hz (1 Hz, 1.83 Hz, 2.66 Hz and 3 Hz on days 1–4, respectively) and maintained at 3 Hz for the remainder of the week (**Supplementary Fig. 1b**; referred to as low-frequency regimen or 3-Hz regimen) or (ii) high-frequency ramp-up regimen, where stimulation started at 1 Hz and increased to 6 Hz throughout the week (1 Hz, 1.83 Hz, 2.66 Hz, 3.49 Hz, 4.82 Hz, 5.15 Hz and 6 Hz; **Supplementary Fig. 1c**; referred to as high-frequency regimen or 6-Hz regimen).

Physiological hypertrophy in stimulated biowires

After 2 weeks in culture, cells throughout the biowires strongly expressed cardiac contractile proteins sarcomeric α-actinin, actin and cardiac troponin T, as evidenced by immunostaining (**Fig. 2a** and **Supplementary Figs. 2** and **3**). Sarcomeric banding

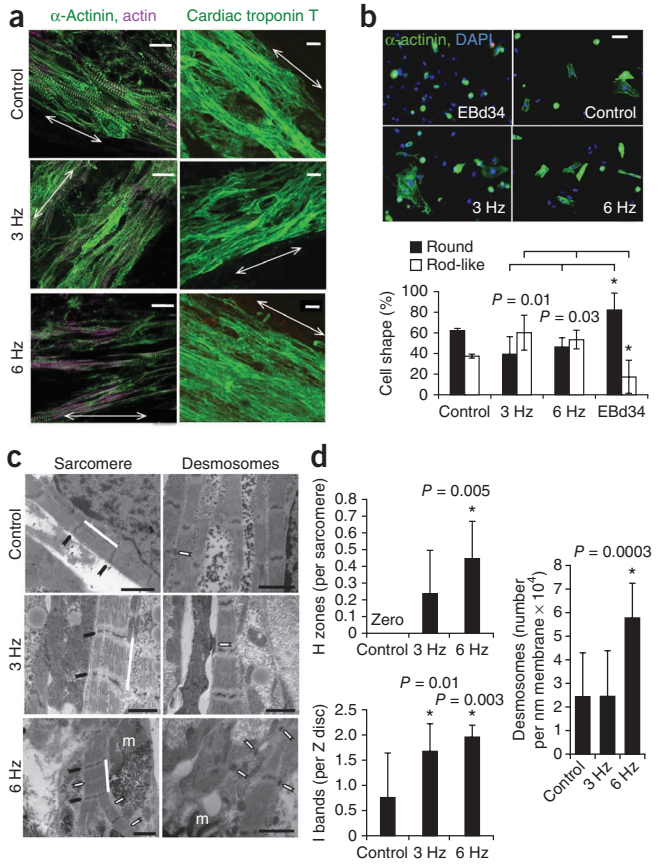

Figure 2 | Cultured biowires in combination with electrical stimulation promoted physiological cell hypertrophy and improved cardiomyocyte phenotype. (**a**) Representative confocal images of nonstimulated (control) and electrically stimulated biowires (3-Hz and 6-Hz regimens) showing cardiomyocyte alignment and frequent Z disks (double-headed arrows represent suture axis). (**b**) Analysis of cardiomyocyte cell shape in indicated conditions (average ± s.d., $n = 3$ per group). EBd34 versus cells subjected to 3-Hz regimen, $P = 0.01$ for both rod-like and round; EBd34 versus 6 Hz, $P = 0.03$ for both round and rod-like. DAPI, 4′,6-diamidino-2-phenylindole. (**c**) Representative ultrastructural images of nonstimulated (control) and electrically stimulated biowires showing sarcomere structure (sarcomere, white bar; Z disks, black arrows; H zones, white arrows; m, mitochondria) and presence of desmosomes (desmosomes, white arrows). Scale bars, 20 μm (**a**), 50 μm (**b**) and 1 μm (**c**). (**d**) Morphometric analysis (average ± s.d.; $n = 4$ per group) showing ratio of H zones to sarcomeres (control versus 6 Hz, $P = 0.005$) ratio of I bands to Z disks (control versus 3 Hz, $P = 0.01$; control versus 6 Hz, $P = 0.003$) and number of desmosomes per membrane length (control versus 6 Hz, $P = 0.0003$). *, significant difference between group and control. In normal adult cells, the ratio of H zones to sarcomeres is 1 and of I bands to Z disks is 2. Data in **a**–**d** were obtained with Hes2 hESC-derived cardiomyocytes.

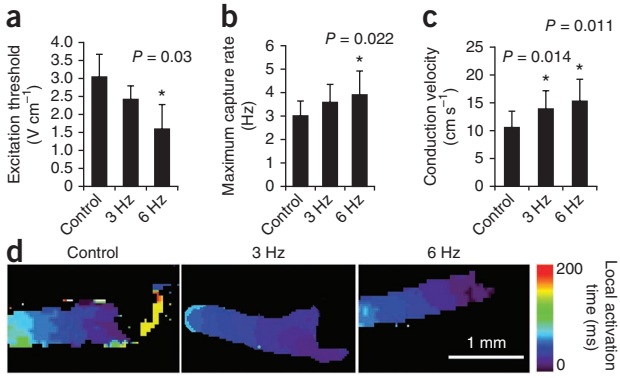

Figure 3 | Functional assessment of engineered biowires. (**a**–**c**) Excitation threshold (**a**; control ($n = 4$) versus cells subjected to 6-Hz regimen ($n = 3$), $P = 0.03$; measured by field stimulation and videomicroscopy; 3 Hz, $n = 3$), maximum capture rate (**b**; control versus 6 Hz ($n = 4$ per group), $P = 0.022$; measured by point stimulation and optical mapping; 3 Hz, $n = 3$) and electrical impulse propagation rates (**c**; control ($n = 13$) versus 3 Hz ($n = 10$), $P = 0.014$; control versus 6 Hz ($n = 5$), $P = 0.011$; measured by point stimulation and optical mapping) after electrical stimulation (average ± s.d.). (**d**) Representative conduction velocity activation maps in biowires. *, significant difference between group and control. Data in **a**–**d** were obtained with hESC-derived cardiomyocytes from Hes2 cell line.

of the contractile apparatus (**Fig. 2a** and **Supplementary Figs. 2c**, **3a** and **4**) and myofibrillar alignment along the suture axis was qualitatively similar to the structure in the adult heart[22]. Biowires kept in culture for 3 weeks and 4 weeks maintained cell alignment and their contractile apparatus structure, as evidenced by confocal and transmission electron microscopy (**Supplementary Fig. 5**).

Early in cardiac development, cardiomyocytes are round cells and differentiate into rod-like cells after birth[24]. Adult human cardiomyocytes have a structurally rigid architecture, retaining a rod-like shape[25] immediately after dissociation, whereas hESC-derived cardiomyocytes remain round. We dissociated age-matched, EBd34 and biowires, and seeded the cells into Matrigel-coated plates (**Supplementary Fig. 1d**). Although ~80% of cardiomyocytes from EBd34 exhibited a round phenotype, this percentage was significantly lower (~50% less) in electrically stimulated samples (**Fig. 2b**). The percentage of rod-like cardiomyocytes was significantly higher (about fourfold) in electrically stimulated biowires (**Fig. 2b** and **Supplementary Fig. 6**) as compared to EBd34.

During development, cardiomyocytes undergo physiological hypertrophy characterized by an increase in cell size followed by changes in sarcomere structure and downregulation of fetal genes[26]. We observed a significant increase in cardiomyocyte size (area of plated cells) in biowire conditions compared to cardiomyocytes from age-matched embryoid bodies (EBd34) (**Supplementary Table 1**; EBd34 versus control, $P = 0.034$; EBd34 versus 3-Hz regimen, $P = 0.003$; EBd34 versus 6-Hz regimen, $P = 0.01$). Atrial natriuretic peptide (NPPA), brain natriuretic peptide (NPPB) and α-myosin heavy chain (MYH6) are proteins highly expressed in fetal cardiomyocytes and upregulated during pathological hypertrophy in diseased adult ventricular cardiomyocytes. Downregulation of the fetal cardiac gene program (*NPPA*, *NPPB* and *MYH6*) in hESC-derived cardiomyocyte biowires (**Supplementary Fig. 7**), compared to age-matched embryoid bodies, in concert with cell-size increase, suggested physiological hypertrophy and a more mature phenotype. Although we observed downregulation of mRNA encoding structural proteins in biowires compared to embryoid bodies, we observed no changes in the amounts of these protein (**Supplementary Results**). Potassium inwardly rectifying channel gene (*KCNJ2*), that has important roles in cell excitability and K^+ homeostasis[27], was upregulated in cells from biowires compared to EBd34 (**Supplementary Fig. 7**).

hESC-derived cardiomyocytes cultured in biowires also exhibted lower proliferation rates than those of embryoid bodies (**Supplementary Fig. 8**; EBd20 versus EBd34, $P = 0.002$; EBd34 versus control, $P = 0.019$; EBd34 versus 3-Hz regimen, $P = 0.016$; EBd34 versus 6-Hz regimen, $P = 0.015$) and the percentage of cardiomyocytes in each condition remained unchanged after culture for 2 weeks (48.2% ± 10.7% average ± s.d.; **Supplementary Fig. 9**). After cultivation, cell composition in biowires was comparable to that in EBd20, specifically $CD31^+$ (2.4% ± 1.5%, endothelial cells[28]), $CD90^+$ (34.4% ± 23%, fibroblasts[28]), calponin$^+$ (35 ± 22%, smooth muscle cells) or vimentin$^+$ (80% ± 22%, nonmyocytes) cells. This suggests that the observed improvements were not related to the induction of a particular cell type in biowires.

Maturation of contractile apparatus

Cells in nonstimulated biowires exhibited well-defined Z discs and myofibrils (**Fig. 2c** and **Supplementary Figs. 3c** and **4**) but no signs of alignment of Z discs. In contrast, biowires stimulated under the high-frequency regimen showed signs of maturation, such as organized sarcomeric banding with frequent myofibrils that converged and displayed aligned Z discs (6-Hz regimen; **Fig. 2c** and **Supplementary Figs. 3c** and **4**), many mitochondria (6-Hz regimen; **Fig. 2c** and **Supplementary Fig. 3c** and **4**) and desmosomes, a molecular complex of cell-cell adhesion proteins (**Fig. 2c**). In the 6-Hz regimen condition, mitochondria were positioned closer to the contractile apparatus than in control or 3-Hz regimen conditions (**Fig. 2c** and **Supplementary Figs. 3c** and **4b**).

Electrically stimulated samples exhibited a sarcomeric organization more compatible with mature cells than with nonstimulated controls as shown by a significantly higher presence of H zones per sarcomere (**Fig. 2d**, control versus 6-Hz regimen, $P = 0.005$; **Supplementary Fig. 3d**, control versus 6-Hz regimen, $P = 0.001$) and I bands per Z disc (**Fig. 2d**, control versus 3-Hz regimen, $P = 0.01$; control versus 6-Hz regimen, $P = 0.003$; **Supplementary Fig. 3d**, control versus 6-Hz regimen, $P = 0.0004$). Biowires stimulated using the 6-Hz regimen also had a significantly higher number of desmosomes per membrane length than did both nonstimulated controls and biowires subjected to the 3-Hz regimen (**Fig. 2d**, $P = 0.0003$). In hiPSC-derived cardiomyocyte biowires, we frequently saw areas with nascent intercalated discs (**Supplementary Fig. 3c** and **4b**). However, the lack of M lines and T tubules, consistent with previous reports[29,30], indicated an absence of terminal differentiation.

Functional assessment of engineered biowires

Electrical stimulation using the 6-Hz regimen improved biowire's electrical properties, leading to a significant decrease in the excitation threshold (**Fig. 3a**; control versus 6-Hz regimen, $P = 0.03$) and an increase in the maximum capture rate (MCR) (**Fig. 3b**,

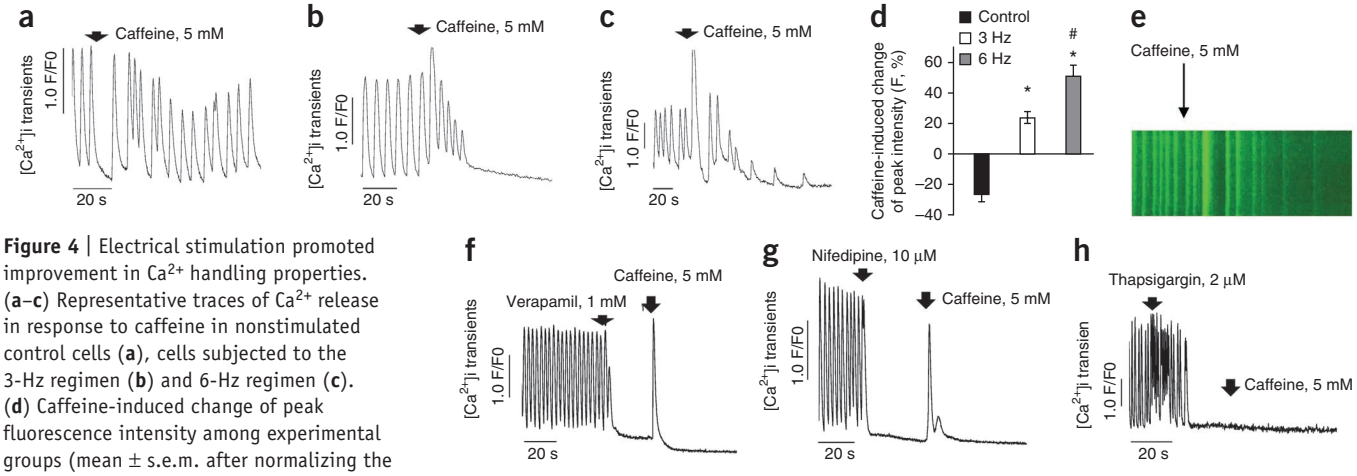

Figure 4 | Electrical stimulation promoted improvement in Ca^{2+} handling properties. (**a**–**c**) Representative traces of Ca^{2+} release in response to caffeine in nonstimulated control cells (**a**), cells subjected to the 3-Hz regimen (**b**) and 6-Hz regimen (**c**). (**d**) Caffeine-induced change of peak fluorescence intensity among experimental groups (mean ± s.e.m. after normalizing the peak fluorescence intensity before administration of caffeine; control versus 3 Hz, $P = 1.1 \times 10^{-6}$; control versus 6 Hz, $P = 2.1 \times 10^{-7}$; 3 Hz versus 6 Hz, $P = 0.003$; $n = 10$ (control), $n = 6$ (3 Hz) and $n = 9$ (6 Hz)). (**e**) Representative fluorescence recording of Ca^{2+} transients before and after administration of caffeine at 5 mM (arrow) in cells subjected to the 6-Hz regimen. (**f**–**h**) Inhibition of L-type Ca^{2+} channels with verapamil (**f**) or nifedipine (**g**) and blockade of SERCA channels with thapsigargin (**h**) in cells subjected to the 6-Hz regimen before addition of caffeine. *, significant difference between group and control. #, significant difference between 3-Hz regimen group and 6-Hz regimen group. Data in **a**–**h** were obtained with hESC-derived cardiomyocytes obtained from Hes2 cell line and represent measurements performed in single cell cardiomyocytes after dissociation from biowires. F, fluorescence intensity; F0, fluorescence intensity at baseline; F/F0, F normalized by F0.

control versus 6-Hz regimen, $P = 0.022$; **Supplementary Figs. 3** and **4**) as analyzed by point stimulation at the end of the cultivation in conjunction with optical mapping of impulse propagation (**Supplementary Fig. 10a** and **Supplementary Videos 2**–**5**). Optical mapping demonstrated higher MCR with field stimulation (5.2 Hz) than with point stimulation (4 Hz) (**Supplementary Fig. 10b**; we observed an MCR of 5.2 Hz with field stimulation and intermittent capture at 6 Hz, **Supplementary Videos 6**–**9**). During field stimulation, all cells received the stimulus at the same time, and response was not limited by each cell's propagation limitations. Conduction velocity, assessed upon point stimulation at the end of cultivation, was ~40% and ~50% higher in the samples electrically stimulated during culture (3 Hz and 6 Hz, respectively), than nonstimulated controls (**Fig. 3c**,**d**, control versus 3 Hz, $P = 0.014$; control versus 6 Hz, $P = 0.011$). Improvements in electrical properties (excitation threshold, MCR and conduction velocity) were more pronounced with the high-frequency regimen compared to the low-frequency one. Improvement in conduction velocity directly correlated with the average number of desmosomes (**Supplementary Fig. 11**, $R^2 = 0.8526$).

Stimulation improves Ca^{2+}-handling properties

Either all[10] or the majority[12] of hESC-derived cardiomyocytes rely on Ca^{2+} influx from sarcolemma rather than on Ca^{2+} release from sarcoplasmic reticulum for contraction, which differs markedly from the case in the adult myocardium. We tested the effect of caffeine, which opens sarcoplasmic reticulum ryanodine channels, on cytosolic Ca^{2+} transients in single cells isolated from biowires (**Supplementary Fig. 1d**). In accordance with previous work[10], none of the hESC-derived cardiomyocytes in nonstimulated controls were responsive to caffeine (**Fig. 4a**), whereas electrically stimulated cells using both 3-Hz and 6-Hz regimen conditions responded to caffeine by inducing an increase in cytosolic Ca^{2+} (**Fig. 4b**,**c**). Quantification of Ca^{2+} transient amplitudes showed that electrically stimulated cells exhibited significantly higher amplitude intensity in response to caffeine than nonstimulated controls, in a stimulation frequency–dependent manner (**Fig. 4d**,**e**). Blockade of L-type Ca^{2+} channels in cells from biowires subjected to the 6-Hz regimen with either verapamil or nifedipine (**Fig. 4f**,**g**) led, as expected in mature cells, to cessation of Ca^{2+} transients. Addition of caffeine after blockade of L-type Ca^{2+} channels led to Ca^{2+} release into the cytosol (**Fig. 4f**,**g**). Blockade of the ion-transport activity of sarcoplasmic reticulum Ca^{2+} ATPase (SERCA) by addition of thapsigargin (**Fig. 4h**) led to the cessation of calcium transients with time because of the depletion of Ca^{2+} from the sarcoplasmic reticulum. Cardiomyocytes from the 6-Hz regimen condition also demonstrated a faster rising slope and time to peak, parameters that represent the kinetics of Ca^{2+} release into the cytosol and faster τ decay and time to base, parameters that represent the kinetics of clearance of Ca^{2+} from the cytosol (**Supplementary Table 2**). Taken together, these data indicated that cardiac biowires stimulated using the 6-Hz regimen during culture exhibited Ca^{2+}-handling properties compatible with a functional sarcoplasmic reticulum.

Stimulation alters electrophysiological properties

To assess maturity, we measured action potentials, human ERG (hERG) currents and inward rectifier currents (I_{K1})[11] in cardiomyocytes derived from biowires and embryoid bodies (**Fig. 5**). hERG currents were larger ($P = 0.0434$) in biowires subjected to the 6-Hz regimen (0.81 pA $pF^{-1} \pm 0.09$ pA pF^{-1}) than nonstimulated controls (0.52 pA $pF^{-1} \pm 0.10$ pA pF^{-1}) (**Fig. 5a**) without differences in their biophysical properties (**Supplementary Fig. 12**). Cardiomyocytes from both biowire groups had higher hERG levels compared to those from day-20 or day-44 embryoid bodies (**Fig. 5a**). Similarly, I_{K1} densities were greater ($P = 0.0406$) in biowires subjected to the 6-Hz regimen (1.53 pA $pF^{-1} \pm 0.25$ pA pF^{-1}) than in controls (0.94 pA $pF^{-1} \pm 0.14$ pA pF^{-1}), and I_{K1} levels in both biowire groups were greater ($P = 0.0005$) than those recorded in embryoid body–derived cardiomyocytes (**Fig. 5b**).

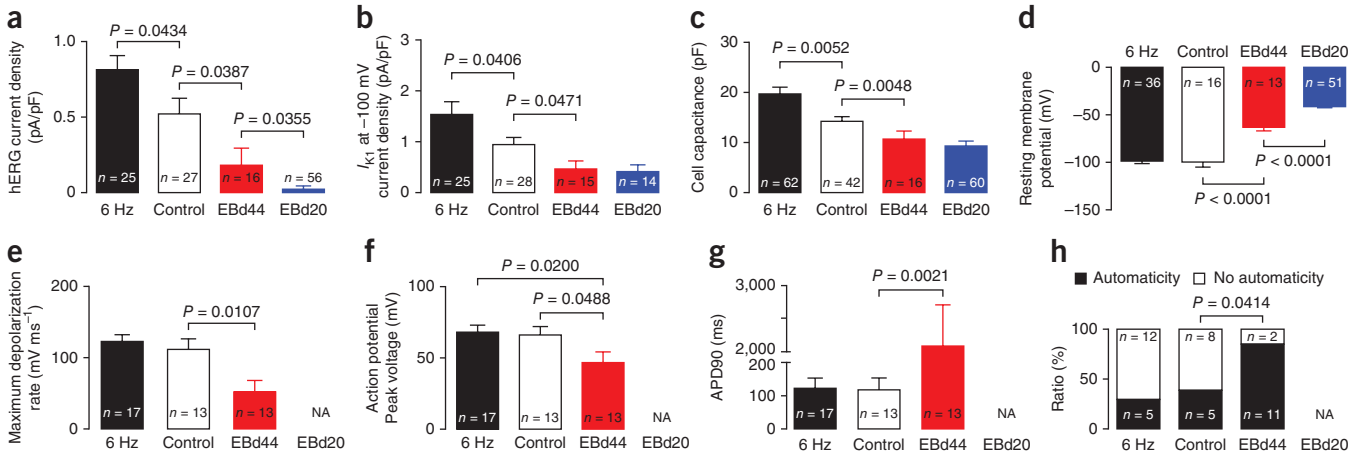

Figure 5 | Electrophysiological properties in single cardiomyocytes isolated from biowires or embryoid bodies and recorded with patch clamp. (**a**) hERG tail current density. (**b**) I_{K1} current density measured at −100 mV. (**c**) Cell capacitance. (**d**) Resting membrane potential. (**e**) Maximum depolarization rate of action potential. (**f**) Action potential peak voltage. (**g**) Action potential duration measured at 90% repolarization (APD90). (**h**) Ratio of cells displaying spontaneous beating (automaticity) or no spontaneous beating (no automaticity). Control, control biowire. Data in **a**–**h** were obtained with hESC-derived cardiomyocytes obtained from Hes2 cell line (average ± s.e.m.).

Cell capacitance, a measure of cell size, was larger ($P = 0.0052$) in biowires subjected to the 6-Hz regimen (19.59 pF ± 1.41 pF) compared to control biowires (14.23 pF ± 0.90 pF) and smaller ($P = 0.0041$) in embryoid body–derived cardiomyocytes (**Fig. 5c**). Resting membrane potentials (V_{rest}) of the cardiomyocytes from biowires were more negative than in embryoid body–derived cardiomyocytes ($P < 0.0001$; **Fig. 5d**). After correcting for the liquid junction potential, which was ~16 mV, the values of V_{rest} recorded in biowire cardiomyocytes with the patch-clamp method were well below the equilibrium potential for Nernst potential for K^+ ($E_K = -96$ mV), suggesting that hyperpolarizing currents, possibly those generated by the Na^+ pump[31,32], strongly influenced V_{rest}. Consistently, we found that the cardiomyocytes from biowires had a very low resting membrane conductance, which correlated with V_{rest} ($R = 0.5584$, $P < 0.0001$), and I_{K1} values had negative correlations with V_{rest} ($R = 0.2267$, $P = 0.0216$; **Supplementary Fig. 13**). Maximum depolarization rates (**Fig. 5e**) and peak voltages of the action potentials (**Fig. 5f**) did not differ between the two biowire groups. However, both properties were improved in these biowire groups compared to embryoid bodies ($P = 0.5248$ and $P = 0.0488$, respectively). Action potential durations were longer ($P = 0.0021$) with greater variation in embryoid body–derived cardiomyocytes than biowire-derived cardiomyocytes (**Fig. 5g** and **Supplementary Fig. 14**), suggesting less electrophysiological diversity and more maturation in biowires. Automaticity (spontaneous beating activity) was greater ($P = 0.0414$) in embryoid body–derived cardiomyocytes compared to control biowires (**Fig. 5h**), which was comparable to that in biowires subjected to the 6-Hz regimen. Taken together, these results support the conclusion that biowires and electrical stimulation using the 6-Hz regimen promoted electrophysiological maturation.

DISCUSSION

Normal human fetal heart rate varies but is maintained at ~3 Hz for most of the time[33] whereas adult resting heart rate is ~1 Hz[33]. The rate change is associated with changes in expression of contractile proteins and suggests a possible dependence of cardiac maturation on stimulation rate. The fact that the progressive increase from 1 Hz to 6 Hz was the best stimulation condition tested in biowires was a surprise to us as 3 Hz is the average fetal heart rate[33]. This could be a compensatory mechanism for the lack of other important cells types and cell-cell developmental guidance in the *in vitro* setting. As we increased frequency of field stimulation over 7 d in culture, the group subjected to the 6-Hz regimen might only lose capture (exceed the rate of 5.2 Hz) at the very last day of stimulation. Therefore, it may be the stimulation at the highest possible rate, and not the rate itself, that is the governing cue for cardiomyocyte maturation *in vitro*.

Mechanical stimulation has been reported to lead to a robust induction of structural proteins such as myosin heavy chain and induce proliferation of hPSC-derived cardiomyocytes[14,34], suggesting that electrical stimulation of the biowire at 6 Hz did not simply provide a better mechanical stimulation environment. Previously, mechanical stimulation did not lead to electrophysiological maturation[34]. The use of electrical stimulation in conjunction with stretch as a mimic of cardiac load[14], concurrently or sequentially, might be required to induce terminal differentiation in hPSC-derived cardiomyocytes and upregulate the expression of myofilament proteins. Other strategies might include cultivation in the presence of T3 thyroid hormone[35], insulin-like growth factor-1 (ref. 36), addition of laminin or native decellularized heart extracellular matrix into the hydrogel mixture[37] and cultivation on stiffer substrates[38,39].

It is well accepted that some human stem cell lines are more cardiomyogenic than others[12,16], and these differences could also be related to the maturity of the produced cells. In previous reports[10,11,40], many and usually most cells were irresponsive to caffeine at the end of differentiation. Therefore, differences in Ca^{2+}-handling properties could also be due to cell line variability. Here we demonstrated that in a given cell line, culture in biowires and electrical-field stimulation enhanced Ca^{2+}-handling properties of cardiomyocytes consistent with a functional sarcoplasmic reticulum.

Biowire cardiomyocytes were clearly more mature than cardiomyocytes obtained from embryoid bodies cultivated for 20 d (EBd20) or for 40–44 d (EBd44), which exhibited a greater propensity for automaticity, more depolarized membrane

potentials, lower cell capacitance and less hERG currents and I_{K1}. Electrophysiological measurements of the EBd20 cardiomyocytes represented the cell properties before their incorporation into biowires, whereas EBd44 cardiomyocytes were cultured for periods slightly longer than the biowire culture time, allowing assessment of the independent effect of culture time on maturation[11,41]. We acknowledge that biowire maturation is clearly incomplete, as evidenced by the relatively low membrane conductance. Nevertheless, it is intriguing to speculate that the combination of low membrane conductance with V_{rest} below E_K may represent an 'intermediate' phenotype as cardiomyocytes undergo maturation from the embryonic state.

Correlating the properties of hPSC-derived cardiomyocytes in biowires with mouse or human development could help to gauge maturation stage, but mouse and rat cardiomyocytes are physiologically distinct, and age-defined healthy human heart samples are scarce. Additionally, *in vitro* maturation might not be compatible with embryo development.

The small size (radius of ~300 µm) of biowire upon gel compaction was selected to be close to the diffusional limitations for oxygen supply to ensure that the biowires can be maintained in culture without perfusion. Addition of vascular cells will be imperative for improving survival and promoting integration with the host tissue in future *in vivo* studies[14]. We generated a unique platform that enables generation of human cardiac tissues of graded levels of maturation that can be used to determine, in future *in vivo* studies, the optimal maturation level that will result in the highest ability of cells to survive and integrate in adult hearts with the lowest side effects (such as arrhythmias).

METHODS

Methods and any associated references are available in the online version of the paper.

Note: Supplementary information is available in the online version of the paper.

ACKNOWLEDGMENTS

We thank P. Lai, C. Laschinger, N. Dubois and B. Calvieri for technical assistance, C.C. Chang and L. Fu for assistance with biowire setup figure preparation. Funded by grants from Ontario Research Fund–Global Leadership Round 2 (ORF-GL2), National Sciences and Engineering Research Council of Canada (NSERC) Strategic Grant (STPGP 381002-09), Canadian Institutes of Health Research (CIHR) Operating Grant (MOP-126027 and MOP-62954), NSERC-CIHR Collaborative Health Research Grant (CHRPJ 385981-10), NSERC Discovery Grant (RGPIN 326982-10), and NSERC Discovery Accelerator Supplement (RGPAS 396125-10) and National Institutes of Health grant 2R01 HL076485.

AUTHOR CONTRIBUTIONS

S.S.N. developed biowire concept, designed and performed experiments, analyzed data and prepared the manuscript. J.W.M. performed experiments and analyzed data. J.L., R.A.-S. and P.H.B. performed patch clamping and microelectrode recordings. Y.X. designed and validated initial device. B.Z. designed and fabricated masters for device fabrication. J.J. and G.J.G. performed calcium transient measurement and analysis. S.M. and K.N. performed optical mapping measurements and analysis. M.G. and G.K. differentiated hESC-derived cardiomyocytes. A.H. designed primers. N.T. developed initial collagen gel mixture. M.A.L. provided training on hiPSC differentiation and cells. P.H.B. contributed to writing of the manuscript. M.R. envisioned the biowire concept and electrical stimulation protocol, supervised the work and wrote the manuscript.

COMPETING FINANCIAL INTERESTS

The authors declare competing financial interests: details are available in the online version of the paper.

1. Kehat, I. *et al.* Human embryonic stem cells can differentiate into myocytes with structural and functional properties of cardiomyocytes. *J. Clin. Invest.* **108**, 407–414 (2001).
2. Yang, L. *et al.* Human cardiovascular progenitor cells develop from a KDR+ embryonic-stem-cell-derived population. *Nature* **453**, 524–528 (2008).
3. Zhang, J. *et al.* Functional cardiomyocytes derived from human induced pluripotent stem cells. *Circ. Res.* **104**, e30–e41 (2009).
4. Kattman, S.J. *et al.* Stage-specific optimization of activin/nodal and BMP signaling promotes cardiac differentiation of mouse and human pluripotent stem cell lines. *Cell Stem Cell* **8**, 228–240 (2011).
5. Carvajal-Vergara, X. *et al.* Patient-specific induced pluripotent stem-cell-derived models of LEOPARD syndrome. *Nature* **465**, 808–812 (2010).
6. Laflamme, M.A. & Murry, C.E. Heart regeneration. *Nature* **473**, 326–335 (2011).
7. Snir, M. *et al.* Assessment of the ultrastructural and proliferative properties of human embryonic stem cell-derived cardiomyocytes. *Am. J. Physiol. Heart Circ. Physiol.* **285**, H2355–H2363 (2003).
8. McDevitt, T.C., Laflamme, M.A. & Murry, C.E. Proliferation of cardiomyocytes derived from human embryonic stem cells is mediated via the IGF/PI 3-kinase/Akt signaling pathway. *J. Mol. Cell Cardiol.* **39**, 865–873 (2005).
9. Mummery, C. *et al.* Differentiation of human embryonic stem cells to cardiomyocytes: role of coculture with visceral endoderm-like cells. *Circulation* **107**, 2733–2740 (2003).
10. Dolnikov, K. *et al.* Functional properties of human embryonic stem cell-derived cardiomyocytes: intracellular Ca^{2+} handling and the role of sarcoplasmic reticulum in the contraction. *Stem Cells* **24**, 236–245 (2006).
11. Doss, M.X. *et al.* Maximum diastolic potential of human induced pluripotent stem cell-derived cardiomyocytes depends critically on I(Kr). *PLoS ONE* **7**, e40288 (2012).
12. Liu, J., Fu, J.D., Siu, C.W. & Li, R.A. Functional sarcoplasmic reticulum for calcium handling of human embryonic stem cell-derived cardiomyocytes: insights for driven maturation. *Stem Cells* **25**, 3038–3044 (2007).
13. Satin, J. *et al.* Calcium handling in human embryonic stem cell-derived cardiomyocytes. *Stem Cells* **26**, 1961–1972 (2008).
14. Tulloch, N.L. *et al.* Growth of engineered human myocardium with mechanical loading and vascular coculture. *Circ. Res.* **109**, 47–59 (2011).
15. Caspi, O. *et al.* Tissue engineering of vascularized cardiac muscle from human embryonic stem cells. *Circ. Res.* **100**, 263–272 (2007).
16. Chien, K.R., Knowlton, K.U., Zhu, H. & Chien, S. Regulation of cardiac gene expression during myocardial growth and hypertrophy: molecular studies of an adaptive physiologic response. *FASEB J.* **5**, 3037–3046 (1991).
17. Frank, D. *et al.* Gene expression pattern in biomechanically stretched cardiomyocytes: evidence for a stretch-specific gene program. *Hypertension* **51**, 309–318 (2008).
18. Kuwahara, K. *et al.* NRSF regulates the fetal cardiac gene program and maintains normal cardiac structure and function. *EMBO J.* **22**, 6310–6321 (2003).
19. Nuccitelli, R. Endogenous ionic currents and DC electric fields in multicellular animal tissues. *Bioelectromagnetics* **1** (suppl.), 147–157 (1992).
20. Henderson, D.J. & Chaudhry, B. Getting to the heart of planar cell polarity signaling. *Birth Defects Res. A Clin. Mol. Teratol.* **91**, 460–467 (2011).
21. Zhao, M., Forrester, J. & McCaig, C. A small, physiological electric field orients cell division. *Proc. Natl. Acad. Sci. USA* **96**, 4942–4946 (1999).
22. Radisic, M. *et al.* Functional assembly of engineered myocardium by electrical stimulation of cardiac myocytes cultured on scaffolds. *Proc. Natl. Acad. Sci. USA* **101**, 18129–18134 (2004).
23. Berger, H.J. *et al.* Continual electric field stimulation preserves contractile function of adult ventricular myocytes in primary culture. *Am. J. Physiol.* **266**, H341–H349 (1994).
24. Borg, T.K. *et al.* Specialization at the Z line of cardiac myocytes. *Cardiovasc. Res.* **46**, 277–285 (2000).
25. Bird, S.D. *et al.* The human adult cardiomyocyte phenotype. *Cardiovasc. Res.* **58**, 423–434 (2003).
26. Frey, N. & Olson, E.N. Cardiac hypertrophy: the good, the bad, and the ugly. *Annu. Rev. Physiol.* **65**, 45–79 (2003).
27. Wang, J., Huang, Y. & Ning, Q. Review on regulation of inwardly rectifying potassium channels. *Crit. Rev. Eukaryot. Gene Expr.* **21**, 303–311 (2011).

28. Dubois, N.C. *et al.* SIRPA is a specific cell-surface marker for isolating cardiomyocytes derived from human pluripotent stem cells. *Nat. Biotechnol.* **29**, 1011–1018 (2011).
29. Lieu, D.K. *et al.* Absence of transverse tubules contributes to non-uniform Ca^{2+} wavefronts in mouse and human embryonic stem cell-derived cardiomyocytes. *Stem Cells Dev.* **18**, 1493–1500 (2009).
30. Baharvand, H., Azarnia, M., Parivar, K. & Ashtiani, S.K. The effect of extracellular matrix on embryonic stem cell-derived cardiomyocytes. *J. Mol. Cell Cardiol.* **38**, 495–503 (2005).
31. De Weer, P., Gadsby, D.C. & Rakowski, R.F. Voltage dependence of the Na-K pump. *Annu. Rev. Physiol.* **50**, 225–241 (1988).
32. Sakai, R., Hagiwara, N., Matsuda, N., Kassanuki, H. & Hosoda, S. Sodium–potassium pump current in rabbit sino-atrial node cells. *J. Physiol.* (*Lond.*) **490**, 51–62 (1996).
33. Arduini, D. *Fetal Cardiac Function* (Parthenon Publishing Group, 1995).
34. Schaaf, S. *et al.* Human engineered heart tissue as a versatile tool in basic research and preclinical toxicology. *PLoS ONE* **6**, e26397 (2011).
35. Chattergoon, N.N. *et al.* Thyroid hormone drives fetal cardiomyocyte maturation. *FASEB J.* **26**, 397–408 (2012).
36. McMullen, J.R. *et al.* The insulin-like growth factor 1 receptor induces physiological heart growth via the phosphoinositide 3-kinase(p110alpha) pathway. *J. Biol. Chem.* **279**, 4782–4793 (2004).
37. Seif-Naraghi, S.B. *et al.* Safety and efficacy of an injectable extracellular matrix hydrogel for treating myocardial infarction. *Sci. Transl. Med.* **5**, 173ra125 (2013).
38. Rodriguez, A.G., Han, S.J., Regnier, M. & Sniadecki, N.J. Substrate stiffness increases twitch power of neonatal cardiomyocytes in correlation with changes in myofibril structure and intracellular calcium. *Biophys. J.* **101**, 2455–2464 (2011).
39. Hazeltine, L.B. *et al.* Effects of substrate mechanics on contractility of cardiomyocytes generated from human pluripotent stem cells. *Int. J. Cell Biol.* **2012**, 508294 (2012).
40. Blazeski, A. *et al.* Electrophysiological and contractile function of cardiomyocytes derived from human embryonic stem cells. *Prog. Biophys. Mol. Biol.* **110**, 178–195 (2012).
41. Lundy, S.D., Zhu, W.Z., Regnier, M. & Laflamme, M. Structural and functional maturation of cardiomyocytes derived from human pluripotent stem cells. *Stem Cells Dev.* Advance online publication 6 March 2013 (doi:10.1089/scd.2012.0490).

ONLINE METHODS

Human pluripotent stem cell culture and differentiation. Cardiomyocytes derived from two different hESC lines (Hes2 and Hes3) and two different hiPSC lines (CDI-MRB and HR-I-2Cr-2R) were used. Both hESC lines and hiPSC line HR-I-2Cr-2R were maintained as described[2,4]. Embryoid bodies (EBs) were differentiated to the cardiovascular lineage as previously described[2,4]. In brief, EBs were generated by culture in StemPro-34 (Invitrogen) medium containing BMP4 (1 ng/ml). On day 1, EBs were collected and suspended in induction medium (StemPro-34 containing basic fibroblast growth factor (bFGF; 2.5 ng/ml), activin A (6 ng/ml) and BMP4 (10 ng/ml)). On day 4, the EBs were collected from the induction medium and recultured in StemPro-34 supplemented with vascular endothelial growth factor (VEGF; 10 ng/ml) and DKK1 (150 ng/ml). On day 8, the medium was changed again and the EBs were cultured in StemPro-34 containing VEGF (20 ng/ml) and bFGF (10 ng/ml) for the duration of the experiment. Cultures were maintained in hypoxic environment (5% CO_2 and 5% O_2) for the first 12 d and then transferred into 5% CO_2 for the remainder of the culture period. EBs were dissociated for seeding in biowires on day 20 (EBd20), day 34 (EBd34) and day 40–44 (EBd44) for specific cellular and electrophysiological analyses. CDI-MRB hiPSC-derived cardiomyocytes were purchased from Cellular Dynamics International (CMC-100-110-001) and used for biowire production immediately after thawing.

Device design and manufacture. The device was fabricated using soft lithography technique. A two-layer SU-8 (Microchem Corp.) master was used to mold PDMS. Briefly, device features were printed on two film masks (CADART) corresponding to the two-layer design. SU-8 2050 was spun onto 4-inch silicon wafer, baked and exposed to UV light under the first-layer mask to create the first layer including the suture channel and the chamber with thickness of 185 μm. The second layer including only the chamber with thickness of 115 μm was spun on top. After additional baking, the second-layer mask was aligned to the features on the first layer and then exposed to UV light. Finally, the wafer was developed using propylene glycol monomethyl ether acetate (Doe & Ingalls Inc.). PDMS was then cast onto the SU-8 master and baked for 2 h at 70 °C. PDMS templates were used to hold a piece of surgical suture centrally in the channel (**Supplementary Fig. 1a**) to which the cardiac cell suspension gel was added.

Biowire generation. EBd20 generated as described above were incubated in collagenase type I (1 mg/ml; Sigma) and DNAse (1 mg/ml, CalBiochem) in Hank's balanced salt solution (NaCl, 136 mM; $NaHCO_3$, 4.16 mM; Na_3PO_4, 0.34 mM; KCl, 5.36 mM; KH_2PO_4, 0.44 mM; dextrose, 5.55 mM and HEPES, 5 mM) for 2 h at 37 °C. EBs were centrifuged (107*g*, 5 min), incubated with trypsin (0.25%, Gibco) for 5 min at 37 °C and pipetted gently to dissociate the cells. After dissociation, cells were centrifuged (167 x g, 5 min), counted and seeded at 0.5×10^6 cells/wire of 0.5 cm in length. This ratio was maintained for generation of longer biowires. Cells were seeded in collagen type I gels (4 μl/0.5 cm wire length; 2.1 mg/ml of rat tail collagen type I (BD Biosciences) in 24.9 mM glucose, 23.81 mM $NaHCO_3$, 14.34 mM NaOH, 10 mM HEPES, in 1× M199 medium plus 10% of growth factor reduced Matrigel (BD Biosciences)) by pipetting the cell suspension into the main channel of the PDMS template (**Supplementary Fig. 1a**). CDI-MRB hiPSC-derived cardiomyocytes were thawed, counted and seeded in same concentration as hESC-derived cardiomyocytes. After seeding, cells were kept in culture for 7 d to allow collagen matrix remodeling and assembly around the suture (**Fig. 1a**,**b**).

Electrical stimulation setup and conditions. After preculture for 7 d, biowires were transferred to stimulation chambers fitted with two 1/4-inch-diameter carbon rods (Ladd Research Industries) placed 2 cm apart and connected to a cardiac stimulator (Grass s88x) with platinum wires (Ladd Research Industries). Biowires were placed perpendicular to the electrodes and were either submitted to electrical stimulation (rectangular, biphasic, 1 ms, 3–4 V/cm) or cultured without electrical stimulation (nonstimulated controls or control) for 7 d (**Supplementary Fig. 1b**,**c**). As increased time in culture affects maturation[11,41], age-matched EBs (EBd34) were used as an additional control. For long-term stimulation experiments, shown in **Supplementary Fig. 5**, the biowires were precultured for 7 d as described above, followed by 7 d of 6-Hz protocol, at which point the frequency was decreased to 1 Hz (to mimic postnatal decrease in heart rate) and maintained for an additional 14 d.

To verify that biowire-stimulated cardiomyocytes truly exhibited maturation on a single-cell basis, assays were performed in which single cells were used. With this goal, biowires were digested with collagenase type I (1 mg/ml; Sigma) and DNAse (1 mg/ml, CalBiochem) in Hank's balanced salt solution (NaCl, 136 mM; $NaHCO_3$, 4.16 mM; Na_3PO_4, 0.34 mM; KCl, 5.36 mM; KH_2PO_4, 0.44 mM; dextrose, 5.55 mM; and HEPES, 5 mM) for 4 h at 37 °C, centrifuged (107*g*, 5 min), incubated with trypsin (0.25%, Gibco) for 5 min at 37 °C and pipetted gently to dissociate the cells as depicted in **Supplementary Figure 1d**. Isolated single cells were seeded on Matrigel-coated or laminin-coated glass coverslips as described below, and area, calcium transient and patch-clamp measurements were performed.

Assessments. The progression of tissue assembly was assessed at various levels after 2 weeks in culture (7 d of gel compaction followed by 7 d of stimulation): functional (excitation threshold, MCR, conduction velocity and Ca^{2+} handling); ultrastructural (sarcomere development, frequency (number/membrane length) of desmosomes), cellular (cell size and shape, proliferation, distribution of cardiac proteins: actin, troponin T and α-actinin), electrophysiological (hERG, I_{K1} and I_{Na}) and molecular (expression of cardiac genes and proteins).

Immunostaining and fluorescence microscopy. Immunostaining was performed using the following antibodies: mouse anti–cardiac troponin T (1:100, Thermo Scientific; MS-295-P1), mouse anti-α-actinin (1:200, Abcam, ab9465), anti-mouse–Alexa Fluor 488 (1:400, Invitrogen, A21202), anti-Ki67 (1:250, Millipore, AB9260), anti-rabbit–TRITC (1:400, Invitrogen, 81-6114). DAPI was used to counterstain nuclei. Phalloidin–Alexa Fluor 660 (1:1,000, Invitrogen, A22285) was used to detect actin fibers. The stained cells were visualized using a fluorescence microscope (Leica CTR6000) and images captured using the Leica Application Suite software. For confocal microscopy, cells were visualized using a fluorescence confocal microscope (Zeiss LSM-510).

doi:10.1038/nmeth.2524

Transmission electron microscopy. Tissue was fixed with 4% paraformaldehyde, 1% glutaraldehyde in 0.1 M PBS for at least 1 h and washed 3 times with PBS pH 7.2. Post-fixation was done with 1% osmium tetraoxide in 0.1 M PBS, pH 7.2 for 1 h and dehydrated using ethanol series from 25% to 100%. Tissue was infiltrated using Epon resin and polymerized in plastic dishes at 40 °C for 48 h. Tissue was stained with uranyl acetate and lead citrate after sectioning. Imaging was performed at Hitachi H-7000 transmission electron microscope.

Optical mapping. Biowires were incubated with a voltage-sensitive dye (Di-4-ANEPPS, 5 μM, Invitrogen) for 20 min at 37 °C in warm Tyrode's solution (118 mM NaCl, 4.7 mM KCl, 1.25 mM $CaCl_2$, 0.6 mM $MgSO_4$, 1.2 mM KH_2PO_4, 25 mM $NaHCO_3$ and 6 mM glucose; oxygenated by bubbling carbogen 95% O_2, 5% CO_2 for at least 20 min shortly before use). Dye fluorescence was recorded on an MVX-10 Olympus fluorescence microscope equipped with a high-speed complementary metal-oxide semiconductor (CMOS) camera (Ultima-L, Scimedia)[42,43]. The 1-cm sensor had 100 × 100 pixel resolution and the spatial resolution was 50–100 μm/pixel. Imaging was performed at 200 frames/s. The fluorescence was excited using a mercury arc source (X-Cite Exacte) with green filter (Olympus U-MWIG2 filter cube). The constructs were electrically point-stimulated using a bipolar electrode made of two fine wires (AWG#32) inserted in a stainless steel needle, which was mounted on a micromanipulator (World Precision Instruments). For electrical field stimulation, the chamber depicted in **Supplementary Figure 1** was used. The plate containing the biowires was placed on a heated plate (MATS-U55S, Olympus) and temperature was regulated at 38 °C. Data analysis was performed using BrainVision software (Scimedia).

Intracellular recordings. Action potentials were recorded in biowires with high-impedance glass microelectrodes (50–70 MΩ, filled with 3 M KCl) at 37 ± 0.5 °C. Biowires were superfused with Kreb's solution containing 118 mM NaCl, 4.2 mM KCl, 1.2 mM KH_2PO_4, 1.8 mM $CaCl_2$, 1.2 mM $MgSO_4$, 23 mM $NaHCO_3$, 20 mM glucose and 2 mM Na-pyruvate, equilibrated with 95% O_2 and 5% CO_2; final pH was 7.4. The microelectrodes were connected to an Axopatch 200B amplifier (Axon Instrument) current clamp. Signals were filtered at 1 kHz, sampled at 2 kHz and analyzed with Clampfit 10 (Axon Instrument). Resting potential was measured at $I = 0$ mode. For some experiments, biowires were paced using field stimulation set at twice the excitation threshold.

Patch-clamp recordings. Single cells isolated from biowires (**Supplementary Fig. 1d**) or EBs were seeded on laminin-coated glass coverslips (laminin, Sigma-Aldrich, 10 μg/cm^2) overnight before patch-clamp experiments were performed. Whole-cell patch-clamp recordings were made using an Axopatch 200B amplifier at room temperature (23–25 °C). Data were analyzed with Clampfit 8.0 (Axon Instrument). Amplifier was set at $I = 0$ when measuring resting potential of cells. Action potentials were recorded by using the current-clamp mode method. Myocytes were stimulated at 1 Hz, and the maximum rate of membrane depolarization, the action potential peak and action potential duration at 90% (APD90) of the 10th action potential were measured. The membrane potentials were not corrected for the liquid junction potentials, which were estimated to be 15.9 mV (estimated with Clampfit 8.0) for the solutions used. Na^+ current, hERG current and I_{k1} current were also recorded under voltage-clamp conditions with 70–80% series resistance compensation. Na^+ current was induced from holding potential of −80 mV by applying a series of test pulses ranging from −120 mV to +30 mV for 500 ms with 10-mV increments followed by a test pulse to −10 mV for 100 ms for measurement of steady-state inactivation. Although this protocol simultaneously activates overlapping voltage-dependent Ca^{2+} currents, these Ca^{2+} currents were estimated (using prepulse protocols) to be less than 3% of the evoked Na^+ currents. hERG was assessed by measuring tail currents in response to steps to −50 mV (for 500 ms) after depolarization to voltage steps ranging from −45 mV to 60 mV with 15-mV increments for 2,000 ms. The peak amplitude of hERG tail current was measured and compared. I_{K1} was measured in two ways that were found to be equivalent for our studies. For complete *I-V* relationships, we assessed Ba^{2+}-sensitive currents by subtracting (trace-by-trace for voltage steps ranging from −120 to −10 mV in 10-mV increments from holding potential of −40 mV) the currents measured in the presence of 500 μM Ba^{2+} from the current measured in the absence of Ba^{2+}. For the purposes of measuring the I_{K1} density, we subtracted the background current from that measured in the absence of Ba^{2+} at −100 mV.

Patch-clamp recordings were performed in bath solutions containing 140 mM NaCl, 4 mM KCl, 1 mM $MgCl_2$, 1.2 mM $CaCl_2$, 10 mM HEPES, 10 mM D-glucose, at pH 7.35 adjusted with NaOH. Pipette resistance was ~5.5–7.5 MΩ when filled with a solution containing 120 mM potassium aspartate, 20 mM KCl, 4 mM NaCl, 1 mM $MgCl_2$, 5 mM MgATP, 10 mM HEPES and 10 mM EGTA, at pH 7.2 adjusted with KOH (calculated reversal potential of K^+ was −95.6 mV after pH adjustment). Dofetilide 100 nM (ref. 44) and $BaCl_2$ 500 μM[11] were used to block hERG current and I_{k1}, respectively.

Calcium transient measurements. Biowires were dissociated by incubation with collagenase and trypsin as described above. The dissociated cardiomyocytes were plated onto 25-mm microscope glass coverslips coated with growth factor–free Matrigel (diluted 1:60 in RPMI medium) and cultured overnight. Cells were then incubated with 5 μM of fluo-4 acetoxymethyl ester (fluo-4 AM) in culture medium for 2 h at 37 °C. Subsequently, cardiomyocytes were washed twice with dye-free medium and placed back into the incubator for 30 min. A laser-scanning confocal microscope (Zeiss LSM 510) was used to measure the fluorescence intensity of fluo-4 AM. The coverslips containing the fluo-4 AM–loaded cardiomyocytes were moved onto a special chamber and tightly secured. Approximately 1.8–1.9 ml of culture medium was added into the chamber, which was placed on a temperature-controlled plate (37 °C) on the microscope. Fluo-4 AM was excited via an argon laser (488 nm), and emitted fluorescence was collected through a 505 nm emission filter. Changes in fluo-4 AM fluorescence intensity, which indicates transient fluctuation of cytosolic calcium concentration, were recorded in frame and line-scan model. The images and fluorescence data were acquired through Zeiss software. The fluorescence data were analyzed with Origin 8.5 software. Fluorescence signals were normalized to baseline fluorescence after loading fluo-4 AM. The rising phase of the signals was fitted by linear model, and the decaying phase of the

signals was fitted by ExpDecay with Offset model. Caffeine, verapamil (Sigma) and fluo-4 AM (Invitrogen) were directly added into the chamber that contained the cardiomyocytes during imaging at concentrations indicated in the figures. Cells beating at similar average beating frequency (9.4 ± 0.7 beats per minute (bpm) for control, 9 ± 0.7 bpm for 3-Hz regimen and 10 ± 0.8 bpm for 6-Hz regimen) were used for calcium transient measurements to ensure that differences in beating rates would not affect the measurements.

Quantitative RT-PCR. RT-PCR was performed as previously described[28]. Total RNA was prepared with the High Pure RNA Isolation Kit (Roche) and treated with RNase-free DNase (Roche). RNA was reverse-transcribed into cDNA using random hexamers and oligo(dT) with SuperScript VILO (Invitrogen). RT-qPCR was performed on a LightCycler 480 (Roche) using LightCycler 480 SYBR Green I Master (Roche). Expression levels were normalized to the housekeeping genes TATA box binding protein (*TBP*) or glyceraldehyde 3-phosphate dehydrogenase (*GAPDH*). The oligonucleotide sequences are summarized in **Supplementary Table 3**.

Flow cytometry analysis. Cells were obtained from biowires or EBs by dissociation with collagenase and trypsin as described above and fixed with 4% paraformaldehyde for 10 min at room temperature. For intracellular epitopes, cells were permeabilized in PBS containing 5% FBS and 0.1% Triton X for 10 min on ice before a blocking step of 5% FBS in PBS for 30 min. Cells were incubated with the following antibodies in blocking buffer on ice for 1 h: anti-CD31-PE (1:100) and anti-CD90-APC (1:500, BD Biosciences, 553373 and 559879, respectively); anti–cardiac troponin T (1:100, Thermo Scientific, MS-295-P1); anti-calponin H1 (1:250, Abcam, ab46794); and anti-vimentin (1:100, Sigma-Aldrich, V6630). Secondary antibodies used were anti-mouse–Alexa Fluor 488 (1:400, Invitrogen, A21202) and anti-rabbit–Cy5 (1:500, Jackson ImmunoResearch, 111-175-144). Owing to the intrinsic variability in the percentage of cardiomyocytes in each assay, the percentage of cells positive for each marker (above the secondary-antibody-only control) was normalized to the starting cell population (EBd20) of each experiment to accurately evaluate whether a change in cell population was occurring.

Western blotting. Biowires were solubilized in (2×) Novex Tris-Glycine SDS sample buffer (Life technologies) and proteins were separated by electrophoresis in Novex Tris-Glycine gels (Life Technologies) and transferred to Biotrace NT (Nitrocellulose, Pall Corp.). Membranes were probed with either anti-myosin heavy chain (total, Abcam, ab15, 1:2,000), Phospholamban 1D11 (gift of A. Gramolini, University of Toronto, 1:5,000) or GAPDH (Millipore, MAB374, 1:10,000) antibodies. Secondary antibodies used were peroxidase-conjugated (DAKO, P0448 or P0447, 1:2000). Membranes were developed with ECL reagent Luminata Classico Substrate (Millipore).

Statistical analysis. Statistical analysis was performed using SigmaPlot 12.0. Differences between experimental groups were analyzed by Student's *t*-test except in **Figure 2b** and **Supplementary Table 1**, where statistics was done using two-way ANOVA. Normality test (Shapiro-Wilk) and pairwise multiple comparison procedures (Holm-Sidak method) were used for two-way ANOVA tests. In **Supplementary Figure 6**, statistics was done using one-way ANOVA on Ranks (pairwise multiple comparison, Dunn's method). In **Figure 5** and **Supplementary Figures 12–14**, differences between experimental groups were analyzed by Student's *t*-test, chi-squared test, ANOVA (pairwise multiple comparisons, Holm-Sidak method). $P < 0.05$ was considered significant for all statistical tests.

42. Nanthakumar, K. *et al.* Optical mapping of Langendorff-perfused human hearts: establishing a model for the study of ventricular fibrillation in humans. *Am. J. Physiol. Heart Circ. Physiol.* **293**, H875–H880 (2007).
43. Witkowski, F.X., Clark, R.B., Larsen, T.S., Melnikov, A. & Giles, W.R. Voltage-sensitive dye recordings of electrophysiological activation in a Langendorff-perfused mouse heart. *Can. J. Cardiol.* **13**, 1077–1082 (1997).
44. Snyders, D.J. & Chaudhary, A. High affinity open channel block by dofetilide of HERG expressed in a human cell line. *Mol. Pharmacol.* **49**, 949–955 (1996).

doi:10.1038/nmeth.2524